Mechanically Robust Anti-Fingerprint Coating on Polycarbonate Substrate

Ye Sun, Rajdeep Singh Rawat, Zhong Chen**

Ye Sun, Prof. Zhong Chen

School of Material Science and Engineering

Nanyang Technological University

Singapore 639798, Singapore

E-mail: ASZChen@ntu.edu.sg

Prof. Rajdeep Singh Rawat

Natural Science and Science Education,

National Institute of Education, Nanyang Technological University,

Singapore 637616, Singapore

E-mail: rajdeep.rawat@nie.edu.sg

* To whom correspondence should be addressed. E-mail: ASZChen@ntu.edu.sg (Z.C.); rajdeep.rawat@nie.edu.sg (R.S.R.)

Abstract

Mechanical robustness is required for a wide range of protective coatings for their long-term usage. It is particularly crucial for the coatings on polymeric substrates to maintain the surface free of contamination such as dust and fingerprint. Here, we have developed an effective fabrication method to prepare amphiphobic anti-fingerprint coating on polycarbonate (PC) substrates. Thin films with porous silicon dioxide (SiO_2) nanoparticles were deposited via pulse laser deposition on plasma pre-treated PC substrate. After the coating is applied, trichloro(1H,1H,2H,2H-perfluorooctyl) silane (PFTS) was assembled on the silica surface. The as-prepared PFTS-treated silica coating is superhydrophobic with water contact angle at 155.2 ± 1.8 ° and highly oleophobic with a contact angle of 133.6 ± 3.3 ° with diiodomethane. The coating also displays excellent adhesion with the PC substrate. The developed room temperature deposition process makes it potentially applicable for other low melting point polymeric substrates towards a wider range of functional surface applications.

Keyword: Superhydrophobic, Oleophobic, Self-cleaning, Anti-fingerprint, Anti-reflection, Polymer substrate

1. Introduction

High light transmittance and surface cleanliness are among the most important and challenging requirements for optical materials such as lenses, screens, and shields. Fingerprints, skin oil residues, dust particles during handling or service [1] are the main sources that affect the transparency and sometimes the aesthetic value of the product. Extensive research on surface modification has been conducted to mitigate the impact of such problems. Surface with highly anti-wetting properties against water and oils, known as superamphiphobic surfaces [2], have generated enormous interest in recent years to enable the surfaces' anti-fingerprint and self-cleaning applications. Nature has inspired us with many examples of superhydrophobic surfaces [3] such as lotus leaves [4, 5], insects' legs [6] and wings [7]. Numerous strategies have been developed to construct superhydrophobic surfaces. However, superamphiphobic surfaces are rather challenging as the surface tension of oils are much lower than water, making it difficult to realize oil-repellent surfaces. Criteria to achieve superamphiphobicity have been discussed in detail by Z. He *et al*. [8]. Rough surface "re-entrant [9-11]" structure was suggested to increase the contact angles with water and oils. Besides the rough surface requirement, lower surface energy is also another critical requirement, which is often achieved by coating comprising of low-energy molecules such as fluorine-based compounds [12, 13]. One of the most challenging issues lies with potential conflict between the requirements for amphiphobicity and transparency [1]. A high degree of surface roughness is desirable for superamphiphobicity, however, the light transmittance will be reduced due to increased light scattering. Therefore, it is rather challenging to retain the required high degree of amphiphobicity without loss in the light transmittance, which is often required for optical lens applications.

Many fabrication methods have been developed to construct superamphiphobic surface on metals [14, 15] and glass [16] via chemical etching [17] to roughen the surface first and then decorate the surface with a low surface energy organic compound. Other methods like sol-gel dip-coating [18, 19] and spray coating [20] were developed to simplify the process by combining the surface roughening and low surface energy decoration steps in one. However, the work on fabricating transparent amphiphobic coating on polymer substrates is rare, due to the low melting point of polymer materials and their inert chemical properties, making some of the existing techniques unsuitable.

Polymeric optical lenses have attracted significant attention, especially for applications in medical and consumer products [21] due to their advantages of light weight, better resistance to mechanical impact, and capability of making into sophisticated shape. Substantial growth in demand of replacing oxide glass with polymer materials has been observed. There is an essential need to functionalize polymer surface with self-cleaning and anti-fingerprint properties while retaining the high light transmittance. However, most of the developed fabrication methods require a high temperature calcination process [22], which is not suitable for the heat sensitive polymeric materials. In addition, mechanical stability, especially the adhesion between coating and the substrate, has always been a major challenge for coatings on polymeric substrates.

In this work, we provide an effective method to fabricate a highly transparent amphiphobic coating on polycarbonate (PC) with superhydrophobicity and high oleophobicity. Nanoporous silica particles film was strongly bonded on PC by pulsed laser deposition at ambient temperature. The room-temperature process makes it possible to modify temperature-sensitive polymeric materials. The as-prepared coating demonstrates excellent anti-reflection, anti-fingerprint, and self-cleaning properties after its surface is decorated with a fluorocarbon compound. Mechanically, the coating exhibits a good stability and strong adhesion to the polymer substrate owing to the pre-deposition plasms treatment.

2. Experimental Section

2.1 Sample Preparation

Coating of silica nanoparticle film

Coating of silica nanoparticle film was performed through a two-step process. Polycarbonate (PC) substrate (size of 1.5 cm × 1.5 cm) was cleaned with ethanol and deionized water for a few cycles prior to the coating. A surface oxygen plasma treatment was done before deposition of the silica nanoparticle film. Solution-cleaned PC substrate was placed inside a radio frequency (RF) plasma tube chamber, which was capacitively coupled with two ring electrodes mounted outside the tube. The chamber was evacuated to a base pressure at 10^{-3} mbar through vacuum pump and then stabilized at 10^{-2} mbar after oxygen gas was supplied into the chamber at flow rate of 2 sccm. Oxygen plasma was activated with 250 W RF power supplied by a 13.56 MHz caeser136 RF generator with an auto-impedance matching unit. The oxygen plasma surface treatment was carried out for 15 min.

Silica nanoparticle film was deposited through a pulse laser deposition (PLD) system in the second step. Silicon target (purchased from S1-Lab Pte Ltd, 99.99%) and the plasma treated PC substrate was placed 5 cm away and facing each other in the deposition chamber. The system was evacuated to 10^{-5} mbar and oxygen gas was then introduced into the chamber at a flow rate of 200 sccm, resulting in a stable chamber pressure of 10^{-2} mbar. Nd:YAG 532 nm laser that was operated at 10Hz with laser pulse fluence of $F = 4.74\, Jcm^{-2}$ focused on the silicon target at a spot size around 5.0×10^{-4} cm^2. The deposition process was carried out for 4 different deposition duration: 10 min, 30 min, 60 min and 90 min.

Decoration of Trichloro(1H,1H,2H,2H-perfluorooctyl) silane

Trichloro (1H,1H,2H,2H-perfluorooctyl) silane (PFTS) ($CF_3(CF_2)_5CH_2CH_2SiCl_3$) was purchased from Sigma Aldrich. The as-prepared silica nanoparticle film was immersed in a 0.1 vol% PFTS in hexane solution for 10 min. The sample was then placed in a drying cabinet at 80 °C for 2 h.

2.2 Material Characterization

JEOL 7600 field emission scanning electron microscope (SEM) was used and operated at 2.0 kV to observe surface morphology. NX10 Park system atomic force microscope (AFM) was used to examine the surface topology as well as to measure surface roughness parameters. Kratos AXIS Supra X-ray Photoelectron Spectrometer (XPS) was used for surface chemical composition analysis. For reference, the binding energy of C 1s peak from sp2-bonded carbon at 284.8 eV was used. Additional surface chemical molecular bonding analysis was performed using Fourier Transformation Infra-Red (FTIR) spectrometer (Perkin Elmer Frontier). A contact angle goniometer (OCA 20 Dataphysic) was used to record static water contact angle (WCA) and oil (diiodomethane) contact angle (OCA) with 5 µL DI water droplet and 3 µL oil droplet, respectively. For the sliding angle measurement, the droplet volume is 10 µL for DI water and 5 µL for oils. A Perkin Elmer Lambda 950 UV-VIS-NIR spectrometer was employed to measure the light transmittance in the visible light wavelength range.

2.3 Mechanical Durability

Abrasion Test (MIL-C-48497 standard)

Surface was rubbed with a cheese cloth pad at a constant force (400-gram weight uniformly distributed on 1.5 cm × 1.5 cm substrates, which corresponds to 26.7 kPa pressure). Rubbing action was applied for 20 times (20 strokes) in each test. Observation under SEM as well as naked eye was carried out after the test to monitor the surface condition.

Adhesion Test (MIL-C-48497 standard)

A cellophane tape was pressed (with an applied pressure around 40 kPa) onto the coating surface first and was then pulled off very slowly at an angle of 45 °. Observation under SEM as well as naked eye was carried out after the test.

Adhesion Test (ASTM-3359 standard)

A sharp steel cutter was used to crosscut the coating surface. Cellophane tape was pressed onto the surface and then slowly pulled off from the surface. Observation under SEM as well as naked eye was carried out after the test to assess the coating performance.

3. Results and discussion

Figure 1 schematically illustrates the procedure of fabricating silica nanoparticle film with PFTS coating on PC surface. The whole process is relatively fast and does not require substrate heating. The pulsed laser deposition of silica film was carried out for 4 different durations: 10 min, 30 min, 60 min and 90 min to study the effect of topography and thickness on the wetting behavior as well as the mechanical durability (**Supporting Information**). 60 min deposition of silica nanoparticle film followed with PFTS coating exhibited best results in terms of surface wetting behavior, transparency, and mechanical abrasion resistance. Therefore, we report the results in this manuscript based on 60 min deposition of silica nanoparticle film with PFTS coating unless otherwise mentioned.

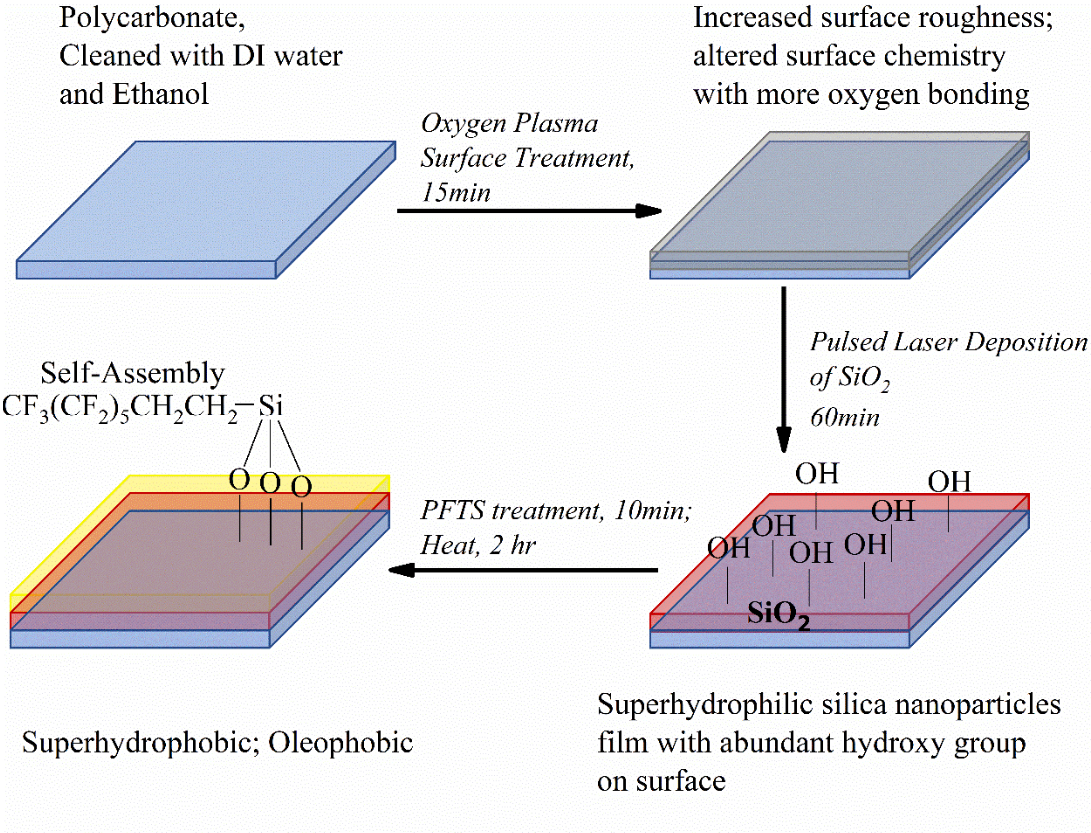

Figure 1. Schematic of fabrication procedures for surface modification on polycarbonate (PC) substrate.

3.1 Surface wettability

Figure 2 shows the static contact angle profiles of water and oil for silica nanoparticle film without and with PFTS coating. The water contact angle (WCA) changed from completely wetting on PLD deposited silica nanoparticle film (**Figure 2a**) to 155.2 ± 1.8 ° (**Figure 2b**) after PFTS decoration. The diiodomethane contact angle (DCA) changed from complete wetting to 133.6 ± 3.3 ° (refer **Figure 2c** and **2d**). The sliding behavior of water and diiodomethane droplets were also tested for silica nanoparticle film with PFTS coating. Significantly low sliding angles for water (approximately 6 °) were observed, while the sliding angles for diiodomethane were around 23 °. A high-speed camera was used to capture droplets sliding off the surface (videos in supporting information). The surface wettability of oil was further evaluated by measuring contact angle of another two oil (Hexadecane, Soybean Oil) shown in **Figure S1**. The surface tension of each oil presented in this work covers relatively a wide range: diiodomethane 48.4 mN m^{-1} [23], soybean oil 31.4 mN m^{-1} [24], Hexadecane 27.1 mN m^{-1} [23]. As-prepared surface exhibits static contact angle all above 90 °. These oils can slide off the surface without leaving any residues behind. Therefore, the coating is superhydrophobic and oleophobic.

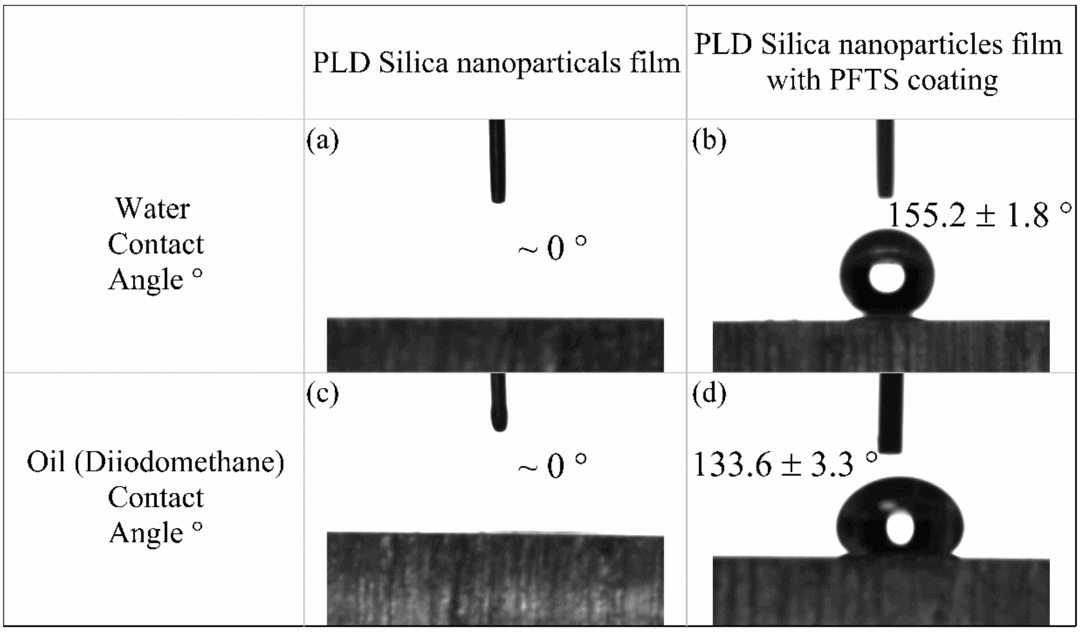

Figure 2. Profiles of water contact angle (WCA) and Oil contact angle (OCA) comparison between (a) (c) silica nanoparticle film and (b) (d) after PFTS coating.

3.2 Surface physical microstructure and chemical structure

Change of the surface property is caused by modification of its physical microstructure as well as the surface chemistry. We used SEM and AFM to characterize the surface physical structures in the current study. XPS was used to detect the surface chemistry composition. SEM and AFM images of as-prepared silica nanoparticle film with PFTS and without PFTS coating are shown in **Figure 3a and b**, respectively. Surface morphology of silica nanoparticle via PLD deposition are well preserved after PFTS coating as similar nanostructures (**Figure 3**) as well as surface roughness (listed in **Table 1**) are observed. As discussed above, it is a great challenge to fabricate anti-fingerprint surface with high optical transmittance, as surface roughness is indispensable for superamphiphobicity. However, high surface roughness may cause light scattering leading to a loss of light transmittance and even appearance (e.g., surface may become milky). A new roughness factor R_f was proposed for theoretical prediction of anti-fingerprint property of the surface coating [25]. The roughness factor is defined as the ratio of arithmetical mean roughness (R_a) over the maximum height (R_v), i.e., $R_f = R_a / R_v$. For lower surface average roughness ($R_a < 1$ μm) surface, relatively deeper valleys (higher R_v) are favored to have better hydrophobic and oleophobic performance. The authors suggested that for an anti-fingerprint surface, R_f should be no greater than 0.2451. This early work provides a guideline on the surface structure to enhance the anti-fingerprint property while retaining high optical transmittance. We carefully modified the surface of pristine PC through oxygen plasma treatment followed by deposition of silica nanoparticles. As shown in the supporting information **Figure S2**, oxygen plasma treatment significantly increases the surface roughness and creates peaks and valleys. Abundant oxygen bonding created by oxygen plasma, as indicated from XPS spectra (**Figure S2**), also helps promote the nucleation and growth [26] of oxide nanoparticles. As shown in **Figure 3**, silica nanoparticles with an average size of 37.4 ±

10.7 nm form clusters in the size of 188.5 ± 36.5 nm are uniformly distributed on the surface without large aggregates. Surface roughness factor R_f was controlled below the recommended value of 0.2451.

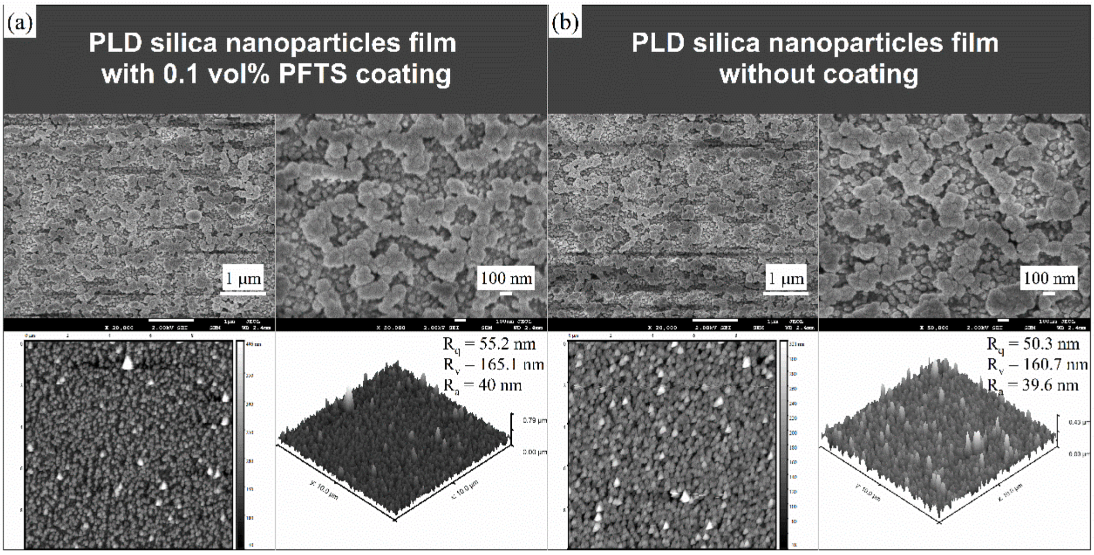

Figure 3. Field emission SEM and AFM images of surface morphology of (a) as-prepared silica nanoparticle film with PFTS coating and (b) without PFTS coating.

Table 1. Roughness measurement comparison between nanoparticle film with PFTS and without PFTS coating.

Roughness	**Silica nanoparticle film with PFTS coating (nm)**	**Silica nanoparticle film without coating (nm)**
$\mathbf{R_q}$	55.2	50.3
$\mathbf{R_v}$	165.1	160.7
$\mathbf{R_a}$	40	39.1
$\mathbf{R_f (R_a/R_v)}$	0.242	0.243

Regarding to the surface chemistry transformation, XPS spectra are shown in **Figure 4**. **Figure 4a** shows the XPS survey spectra of pristine PC, silica film and PFTS coated silica films.

Significant increase of surface oxygen peak as well as the presence of silicon peak (located at 103.4 eV shown in **Figure 4d** for high resolution spectra of Si 2p) after PLD deposition demonstrate that the silica film was coated on PC. The surface of silica is known [27] to be intrinsically hydrophilic due to the presence of the silanol (Si-OH) groups. Silanol group have strong affinity with water through the formation of hydrogen bonds which results in formation of hydrophilic nanoparticle film on surface. The abundant hydroxyl groups (-OH) also provide chemical reaction sites with PFTS. The doublet peaks of C 1s located at 291.1 eV, 293.4 eV and F 1s peak located at 688.2 eV as shown in high resolution spectra **Figure 4b** and **4e** are characterized as $-CF_2$ and $-CF_3$ bond, which clearly indicate the successful deposition of PFTS on top of the silica film. The decoration of the fluorocarbon molecules results in the necessary lower surface energy needed for amphiphobicity.

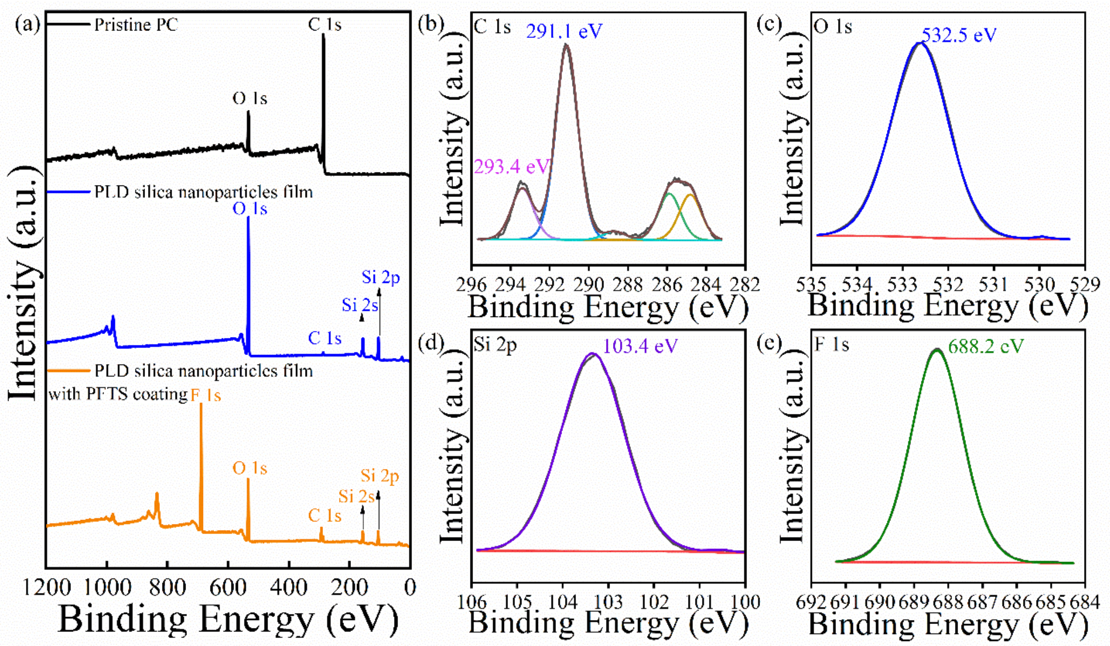

Figure 4. XPS spectra of PFTS coated silica nanoparticle film on polycarbonate substrate (**a**) Survey XPS spectra comparison between pristine PC, silica film and PFTS coated silica film; (**b**) (**c**) (**d**) and (**e**) are high resolution fitted XPS spectra of C 1s, O 1s, Si 2p and F 1s of PFTS coated silica film.

3.3 Surface transparency, self-cleaning and anti-fingerprint property

Figure 5a shows the digital image of as-prepared transparent PC substrate with PTFS coated silica film with water and oil droplets stably standing on the surface. The transmittance measured in the visible wavelength range 400 nm to 700 nm clearly indicates slight increase in light transmittance (shown in **Figure 5b**). The average transmittance between wavelength 400 nm to 700 nm increases from 84.9% to 87.8%. Despite the slight increase in surface roughness there is no increase in the scattering of light as the surface features are much below the wavelength of visible light. On the contrary, the transmittance has increased with the silica nanoparticles coating, which indicates its anti-reflective characteristic. This can be explicated through a single-layered anti-reflection film system [28], in which coating material with a lower refractive index than substrate is preferable. In our study, the silica film is porous and could be treated as a composite of silica and air [29]. This composite would lead to a considerably lower refractive index than silica dense film. Therefore, as-prepared silica nanoparticle film displays anti-reflective performance. Effect of deposition duration on the light transmittance is reported in supporting information.

Figure 5c and **5d** demonstrate anti-fingerprint performance. Fingerprints were created by holding thumb on surface for 2 s with ~100-gram force applied. Comparing the digital image and microscopic image, it is clearly shown that fingerprints stick on pristine PC surface but not on coated PC surface.

The self-cleaning performance can be demonstrated through the removal of contaminants such as dust, dirt, and grease from solid surfaces [30]. In our study, self-cleaning properties of the samples were investigated with titanium oxide powders as the model contaminant particles. As shown in **Figure 5e** and **5f**, titanium oxide powder was uniformly spread on the inclined PC surface. After dripping the water droplets, the silica nanoparticle film with PFTS coating demonstrates strong self-cleaning capability. The water droplets rolled off the superhydrophobic surface and immediately remove the powder along the path. As a comparison, the powder remains on pristine PC surface.

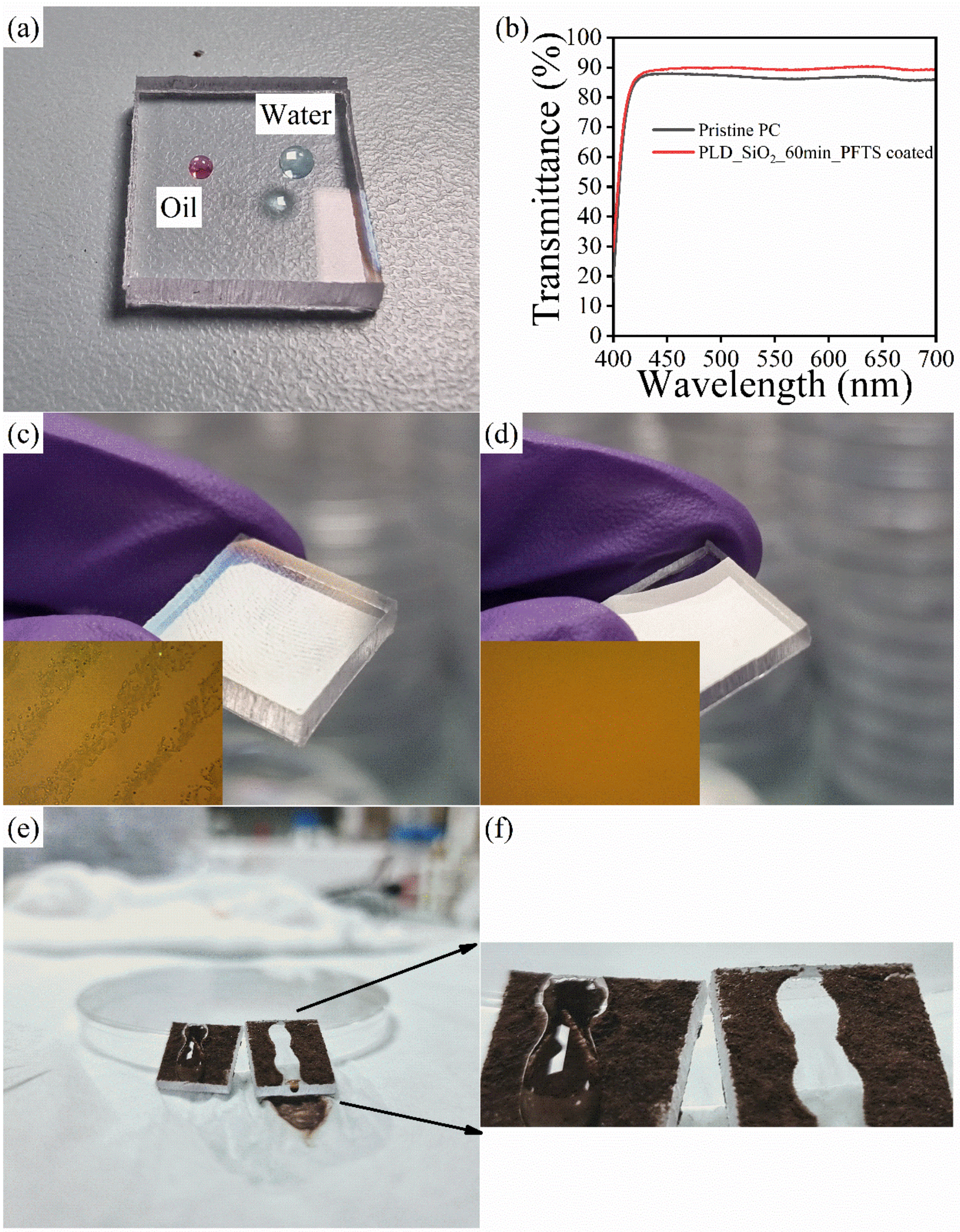

Figure 5. (**a**) The as-prepared PFTS coated silica nanoparticle film shows transparency with repellence of water and oil; (**b**) Light transmittance measured with UV-vis spectrometer; Digital image of presenting transparency anti-fingerprint property (**c**) Pristine PC with fingerprint and (**d**) PFTS coated silica nanoparticle film without fingerprint; (**e**) and (**f**) Self-cleaning process for pristine PC and silica nanoparticle film /PFTS coated PC.

3.4 Mechanism of surface superhydrophobicity and oleophobicty

Figure 6 illustrates the physical and chemical changes in each process step. Oxygen surface plasma treatment not only increases the roughness of the PC substrate surface but also chemically modifies the surface with more oxygen bonding, which promotes nucleation and growth of silica nanoparticles into desire morphology. Furthermore, due to such surface physical and chemical change by oxygen plasma, the adhesion strength of subsequently deposited nanoparticle film has significantly improved. Silica nanoparticle film deposited through pulse laser deposition exhibited superhydrophilicity as there is a large number of hydroxy groups on the surface. During the self-assembly of the PFTS molecules onto the silica nanoparticle surface, chemical reaction between PFTS and Si–OH groups on the surface occurs as evidenced by XPS analysis above. Abundant low surface energy -CF_2 and -CF_3 functional groups on the surface low the surface energy and leads to the superhydrophobicity and oleophobicity with the presence of nano-sized pores.

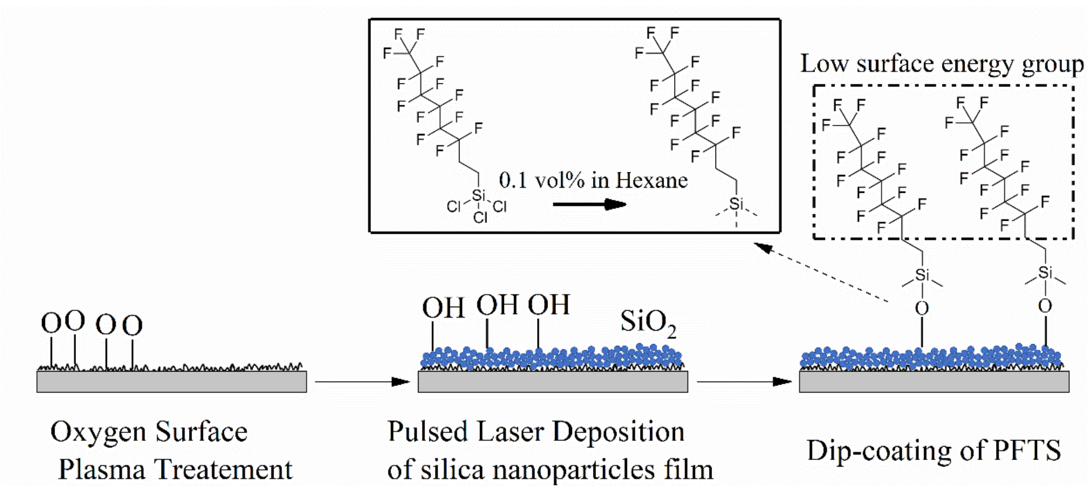

Figure 6. Schematic illustration on the mechanism of surface superhydrophobicity and oleophobicity

3.5 Mechanical robustness and durability of PFTS coated silica coating

Major issues for many practical applications of the coatings are their mechanical reliability and durability. We analyze the coatings' mechanical robustness in our research by measuring coating adhesion and abrasion resistance using US Military Standards (MIL-C-48497). This specification is the most appropriate for optical coatings. Due to the superhydrophobic nature of the coating, the tape displays very weak or no adhesion to the substrate. Therefore, crosshatch test following the ASTM standard was also performed to evaluate the quality of the coating and its adhesion with the substrate. **Figure 7a** shows no coating delamination or chipping along the crosshatched lines which indicates good coating quality and strong coating adhesion with the substrate.

Coating durability was further evaluated by rubbing the surface using a cheese cloth pad as described earlier. Surface morphology was altered (**Figure 7b**) by the applied rubbing action. As indicated in **Figure 7c**, surface roughness is reduced as high peaks and valleys were damaged by the applied shear force during the abrasion. Therefore, surface wettability is affected showing a drop of WCA to 129.2 ± 4.4° and DCA (diiodomethane) to 98 ± 2.6° as indicated in **Figure 7d**. As indicated in transmittance measurement in **Figure 7e**, although a slight drop of average transmittance was observed, higher average transmittance than prinstine PC were still achieved. Despite the drop in the water and oil contact angles, **Figure 7f** shows reduced fingerprints on the surface after the rubbing test when compared with the pristine PC substrate. This means the anti-fingerprint property was largely retained.

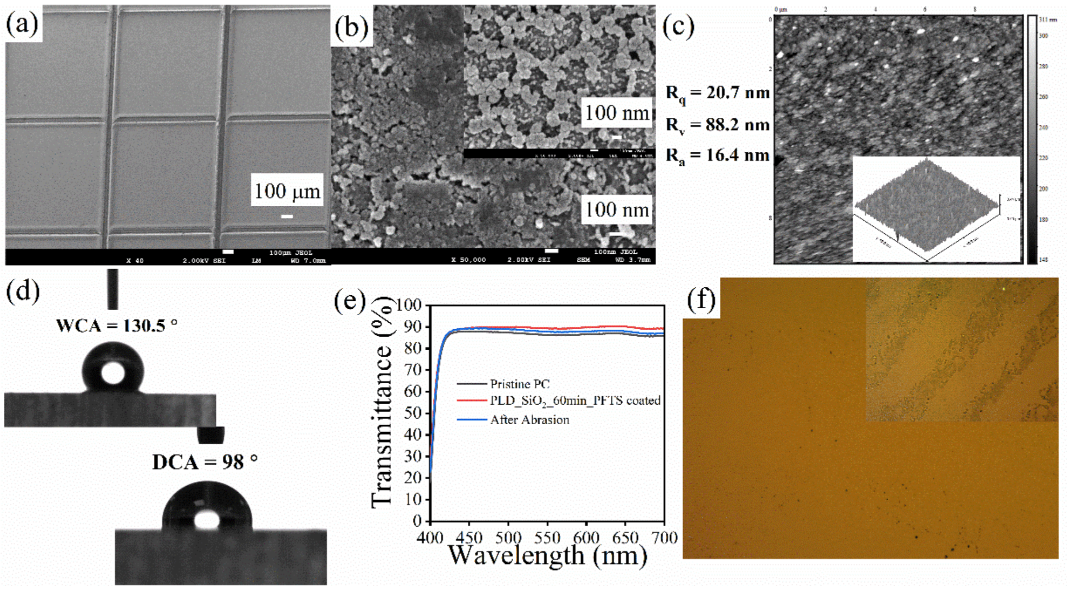

Figure 7. (**a**) Field emission SEM image of crosshatched as-prepared coated PC surface; (**b**) Field emission SEM image of PC surface after abrasion test. Insert is the field emission SEM image of as-prepared coating as comparison. (**c**) AFM topography image and surface roughness measurement for coated PC surface after abrasion testing; (**d**) WCA and OCA after abrasion test; (**e**) Transmittance measurement comparison between as-prepared coated PC and after abrasion test; (**f**) Microscopic image of fingerprint on PC surface after abrasion test. Insert is microscopic image of fingerprint on surface without coating.

4. Conclusion

In this study, we have developed an effective method to prepare a highly transparent and amphiphobic coating with self-cleaning and anti-fingerprint properties. Room temperature deposition of nanoporous silica film by pulse laser deposition created the desirable surface morphology. The functionalization of silica nanoparticles by the low surface energy PFTS molecules was confirmed by the presences of C-F bonds shown in XPS analysis. Oxygen plasma treatment of PC substrate has not only promoted the nucleation and growth of silica nanoparticles into desire morphology, but also enhanced the adhesion between the coating and the substrate. Effect of topography and film thickness on wettability, as well as film durability, was discussed to provide a design insight of constructing such highly transparent amphiphobic coatings.

Combination of the enhanced transparency, superhydrophobic/oleophobic character, and the excellent mechanical durability and adhesion present a great potential for such coating for contaminant-sensitive optical and display applications.

Author contributions

Z.C. and R.S.R. conceived topic. Y.S. performed the experiments, analyzed the results, and drafted the manuscript. Z.C. and R.S.R. revised the manuscript.

Conflict of Interest

The authors declare no conflict of interest.

Funding: Authors gratefully acknowledge financial support in forms of research grants from the Ministry of Education, Singapore (RG16/18, RG8/21) and National Institute of Education (RS 6/18 RSR).

Acknowledgements

The characterization equipment was provided by the Facility for Analysis Characterization Testing & Simulation (FACTS) lab, Nanyang Technological University.

Reference

[1] M. Belhadjamor, M. El Mansori, S. Belghith, S. Mezlini, Anti-fingerprint properties of engineering surfaces: a review, Surface Engineering, 34 (2018) 85-120.

[2] A.K. Kota, G. Kwon, A. Tuteja, The design and applications of superomniphobic surfaces, NPG Asia Materials, 6 (2014) e109-e109.

[3] S.Y. Lee, Y. Rahmawan, S. Yang, Transparent and Superamphiphobic Surfaces from Mushroom-Like Micropillar Arrays, ACS Applied Materials & Interfaces, 7 (2015) 24197-24203.

[4] K. Koch, B. Bhushan, W. Barthlott, Multifunctional surface structures of plants: An inspiration for biomimetics, Progress in Materials Science, 54 (2009) 137-178.

[5] C. Neinhuis, W. Barthlott, Characterization and Distribution of Water-repellent, Self-cleaning Plant Surfaces, Annals of Botany, 79 (1997) 667-677.

[6] X. Gao, L. Jiang, Water-repellent legs of water striders, Nature, 432 (2004) 36-36.

[7] Y. Zheng, X. Gao, L. Jiang, Directional adhesion of superhydrophobic butterfly wings, Soft Matter, 3 (2007) 178-182.

[8] Z. He, M. Ma, X. Lan, F. Chen, K. Wang, H. Deng, Q. Zhang, Q. Fu, Fabrication of a transparent superamphiphobic coating with improved stability, Soft Matter, 7 (2011) 6435-6443.

[9] A. Tuteja, W. Choi, J.M. Mabry, G.H. McKinley, R.E. Cohen, Robust omniphobic surfaces, Proceedings of the National Academy of Sciences, 105 (2008) 18200-18205.

[10] A. Marmur, From Hygrophilic to Superhygrophobic: Theoretical Conditions for Making High-Contact-Angle Surfaces from Low-Contact-Angle Materials, Langmuir, 24 (2008) 7573-7579.

[11] A. Tuteja, W. Choi, M. Ma, J.M. Mabry, S.A. Mazzella, G.C. Rutledge, G.H. McKinley, R.E. Cohen, Designing superoleophobic surfaces, Science (New York, N.Y.), 318 (2007) 1618-1622.

[12] C. Aulin, J. Netrval, L. Wågberg, T. Lindström, Aerogels from nanofibrillated cellulose with tunable oleophobicity, Soft Matter, 6 (2010) 3298-3305.

[13] T. Darmanin, E. Taffin de Givenchy, S. Amigoni, F. Guittard, Hydrocarbon versus Fluorocarbon in the Electrodeposition of Superhydrophobic Polymer Films, Langmuir, 26 (2010) 17596-17602.

[14] N. Valipour Motlagh, F.C. Birjandi, J. Sargolzaei, N. Shahtahmassebi, Durable, superhydrophobic, superoleophobic and corrosion resistant coating on the stainless steel surface using a scalable method, Applied Surface Science, 283 (2013) 636-647.
[15] S. Peng, W. Deng, A simple method to prepare superamphiphobic aluminum surface with excellent stability, Colloids and Surfaces A: Physicochemical and Engineering Aspects, 481 (2015) 143-150.
[16] V.A. Ganesh, S.S. Dinachali, A.S. Nair, S. Ramakrishna, Robust Superamphiphobic Film from Electrospun TiO2 Nanostructures, ACS Applied Materials & Interfaces, 5 (2013) 1527-1532.
[17] H.-J. Choi, J.-H. Shin, S. Choo, S.-W. Ryu, Y.-D. Kim, H. Lee, Fabrication of superhydrophobic and oleophobic Al surfaces by chemical etching and surface fluorination, Thin Solid Films, 585 (2015) 76-80.
[18] Q.F. Xu, J.N. Wang, K.D. Sanderson, Organic−Inorganic Composite Nanocoatings with Superhydrophobicity, Good Transparency, and Thermal Stability, ACS Nano, 4 (2010) 2201-2209.
[19] R.V. Lakshmi, T. Bharathidasan, B.J. Basu, Superhydrophobic sol–gel nanocomposite coatings with enhanced hardness, Applied Surface Science, 257 (2011) 10421-10426.
[20] B.J. Basu, V. Dinesh Kumar, C. Anandan, Surface studies on superhydrophobic and oleophobic polydimethylsiloxane–silica nanocomposite coating system, Applied Surface Science, 261 (2012) 807-814.
[21] W. Beich, Injection molded polymer optics in the 21st-Century, SPIE, 2005.
[22] X. Deng, L. Mammen, H.J. Butt, D. Vollmer, Candle soot as a template for a transparent robust superamphiphobic coating, Science (New York, N.Y.), 335 (2012) 67-70.
[23] Y. Lai, H. Zhou, Z. Zhang, Y. Tang, J.W.C. Ho, J. Huang, Q. Tay, K. Zhang, Z. Chen, B.P. Binks, Multifunctional TiO2-Based Particles: The Effect of Fluorination Degree and Liquid Surface Tension on Wetting Behavior, Particle & Particle Systems Characterization, 32 (2015) 355-363.
[24] S.N. Sahasrabudhe, V. Rodriguez-Martinez, M. O'Meara, B.E. Farkas, Density, viscosity, and surface tension of five vegetable oils at elevated temperatures: Measurement and modeling, International Journal of Food Properties, 20 (2017) 1965-1981.
[25] L.Y.L. Wu, S.K. Ngian, Z. Chen, D.T.T. Xuan, Quantitative test method for evaluation of anti-fingerprint property of coated surfaces, Applied Surface Science, 257 (2011) 2965-2969.
[26] N.T.K. Thanh, N. Maclean, S. Mahiddine, Mechanisms of Nucleation and Growth of Nanoparticles in Solution, Chemical Reviews, 114 (2014) 7610-7630.

[27] L.T. Zhuravlev, Surface characterization of amorphous silica—a review of work from the former USSR, Colloids and Surfaces A: Physicochemical and Engineering Aspects, 74 (1993) 71-90.
[28] H.K. Raut, V.A. Ganesh, A.S. Nair, S. Ramakrishna, Anti-reflective coatings: A critical, in-depth review, Energy & Environmental Science, 4 (2011) 3779-3804.
[29] W. Shimizu, Y. Murakami, Microporous Silica Thin Films with Low Refractive Indices and High Young's Modulus, ACS Applied Materials & Interfaces, 2 (2010) 3128-3133.
[30] A. Eshaghi, Fabrication of transparent silica-silica nanotube/PFTS nano-composite thin films with superhydrophobic, oleophobic, self-cleaning and anti-icing properties, Optical and Quantum Electronics, 52 (2020) 516.